

CZECH TECHNICAL UNIVERSITY IN PRAGUE,  
FACULTY OF ELECTRICAL ENGINEERING

B2MPROJ6 - THESIS PROJECT

---

# Inductive Wireless Power Transfer

---

*Author*

M. ŠIMÁK

DEPARTMENT OF  
ELECTROMAGNETIC FIELD

*Supervisor*

Ing. J. KRAČEK, Ph.D.

DEPARTMENT OF  
ELECTROMAGNETIC FIELD



February 2024

[THIS PAGE INTENTIONALLY LEFT BLANK.]

# Contents

<b>Introduction</b>	<b>2</b>
<b>1 Introduction to inductive wireless power transfer</b>	<b>3</b>
1.1 Equivalent circuit analysis . . . . .	3
<b>2 Simulation of IWPT systems</b>	<b>5</b>
2.1 Simulation results . . . . .	5
2.2 Analytical results . . . . .	6
2.2.1 Resistance . . . . .	6
2.2.2 Inductance . . . . .	7
<b>Conclusion</b>	<b>8</b>
<b>Bibliography</b>	<b>9</b>

# Introduction

In recent years, the landscape of wireless power transfer (WPT) has undergone a significant transformation, fueled by the growing demand for convenient and efficient energy transfer methods in various industries. Among the plethora of wireless power transfer technologies, inductive wireless power transfer (IWPT) has emerged as a promising solution, particularly in the automotive sector. This project aims to delve into the fundamentals of inductive wireless power transfer, focusing on key aspects such as basic configuration, simulation of resistance and inductance, and a comparative analysis of simulation results against analytical formulae.

The automotive industry is undergoing a paradigm shift towards electric vehicles (EVs) and the integration of advanced technologies. As vehicles become more electrified, the demand for efficient and seamless methods of charging electronic devices within the vehicle, such as mobile phones, has intensified. Inductive wireless power transfer, characterized by the transmission of energy through magnetic fields, has garnered attention for its potential to provide a convenient and cable-free charging experience. This project addresses the burgeoning need for a deeper understanding of IWPT systems and their design parameters.

**Synopsis.** In **Chapter 1**, we aim to explore the basic configuration of inductive wireless power transfer systems. This chapter also introduces the tools for analysis of IWPT systems, such as equivalent circuit models.

**Chapter 2** conducts simulations of resistance and inductance using ANSYS Maxwell software, with a particular focus on zero frequency (DC) scenarios. Further on, we compare simulation results with analytical formulae to validate the accuracy and reliability of the simulation model.

**Methodology.** The research methodology involves a step-by-step exploration of inductive wireless power transfer, starting with a theoretical foundation and progressing to detailed simulations using ANSYS Maxwell software. The comparison of simulation results with analytical formulae will provide a rigorous validation process.

# 1. Introduction to inductive wireless power transfer

Wireless power transfer (WPT) in general is a mechanism which can be intermediated by the means of various technologies operating at different power levels and feasible distances. These technologies include far-field WPT which can be implemented by adopting an acoustic, optical or electromagnetic wave as the energy carrier. On the other hand, there are various near-field techniques utilizing the inductive coupling effects of non-radiative electromagnetic fields. The emphasis of this document is on the inductive variant due to its higher efficiency and thus industrial applicability.

This chapter delves into the foundational aspects of IWPT systems. The primary objective is to elucidate the basic configurations employed in IWPT technology. Furthermore, this chapter introduces crucial analytical tools essential for understanding and optimizing IWPT systems, notably equivalent circuit models.

## 1.1 Equivalent circuit analysis

In general, a wireless power transmission chain from source to appliance can be rather complex and its in-depth investigations have been published, such as the power balance in [1]. The circuit model of the inductive transmission chain is depicted in Figure 1.1 along with the matching network on the side of the source and complex load representing the appliance energy sink.

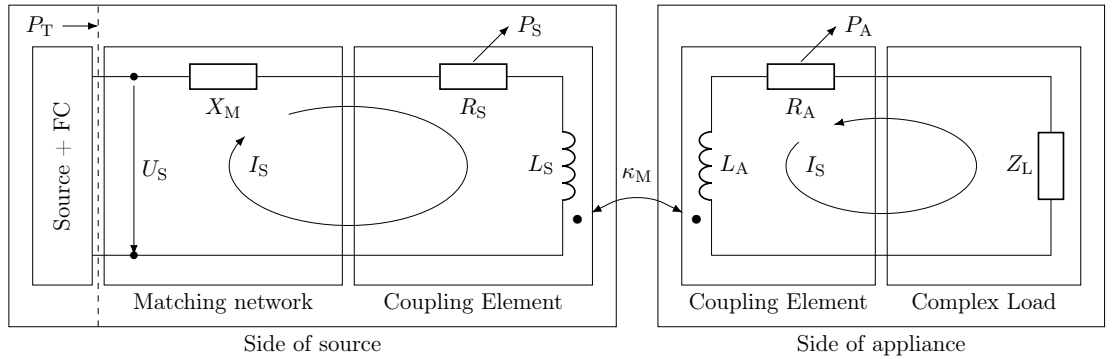


Figure 1.1: Circuit model of a transmission chain

The mutually coupled inductors in the centre of Figure 1.1 can be redrawn using an equivalent circuit model as depicted in Figure 1.2. Here, the coupling coefficient between the transmitting and receiving coils  $\kappa_M$  is represented by the mutual inductance:

$$\kappa_M = \frac{M}{\sqrt{L_S L_A}}. \quad (1.1.1)$$

Understanding inductive coupling in IWPT systems is paramount due to its pivotal role in enabling efficient energy transfer between coils. As depicted in Figure 1.1, the mutual electromagnetic induction between the transmitter and receiver coils forms the core mechanism of IWPT. This coupling phenomenon determines the efficiency and reliability of power transfer, making it imperative for thorough investigation.

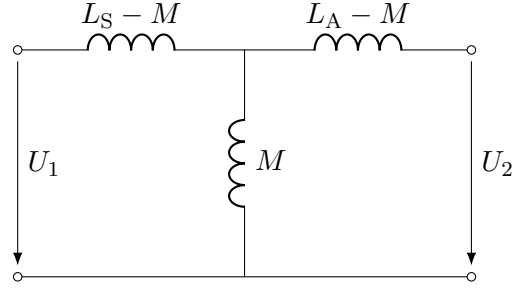


Figure 1.2: Mutually coupled inductors – equivalent circuit

Furthermore, Figure 1.1 highlights the significance of equivalent circuit analysis in comprehending inductive coupling. By abstracting the intricate interactions between coils into simplified models, equivalent circuits, such as the model in Figure 1.2, provide a systematic framework for analyzing IWPT systems. Parameters such as impedance matching, resonance frequency, and power transfer efficiency, depicted in the equivalent circuit representation, offer crucial insights into system performance.

In the following chapter, we perform a 3D CAD simulation applied to the basic configuration of coupled inductors, providing an approach for determining the values of resistances and inductances crucial to Figure 1.1.

## 2. Simulation of IWPT systems

In this chapter, we delve into the simulation aspects of IWPT systems using *Maxwell ANSYS* software. The focus of this investigation is on the simulation of basic coupled inductors, serving as a fundamental model for IWPT systems. Through these simulations, we aim to extract key parameters such as self and mutual inductance, as well as the DC resistance of both the transmitting and receiving coils.

One of the primary objectives of this simulation study is to validate the accuracy of the simulated parameters against analytical formulae. By comparing the simulated values of self and mutual inductance, as well as DC resistance, with their analytically derived counterparts, we aim to assess the fidelity of the simulation model and its ability to capture the behavior of IWPT systems.

### 2.1 Simulation results

The simulation process involves setting up the geometries and material properties of the coils within the software environment, accurately representing the physical characteristics of the inductive components. By applying appropriate boundary conditions and excitation sources, we replicate the operational conditions of IWPT systems to obtain realistic results.

For the validation of simulation results, we can construct a 3D CAD model of the basic IWPT configuration: coupled inductors. This model can be seen in Figure 2.1 with terminals reaching outside the figure to the edge of the simulation space. The bounding box dimensions must always be chosen great enough to encompass the vast majority of the excited field in order to minimize the numerical error caused by cutting off the simulation space. For the excitation of 1 A applied to the terminals, a bounding cube with an edge of 200 mm is sufficient for practical compliance with reality.

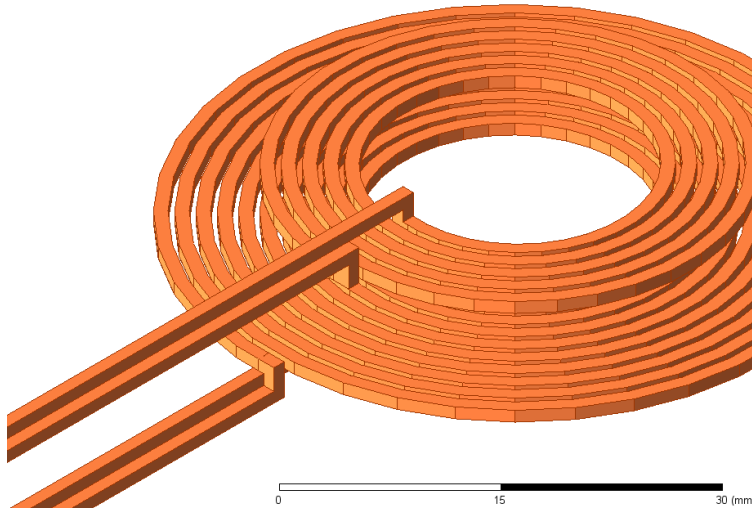


Figure 2.1: Basic coupled inductors

Performing analysis of the 3D CAD model in *Maxwell ANSYS*, we can extract

the values of resistance along with self and mutual inductance.<sup>1</sup> In more detail, the simulation results of the DC resistance are

$$R_{\text{Tx}} = 21.7 \text{ m}\Omega, \quad R_{\text{Rx}} = 10.5 \text{ m}\Omega. \quad (2.1.1)$$

Furthermore, the simulated DC inductance values are

$$L_{\text{Tx}} = 3.8 \text{ }\mu\text{H}, \quad L_{\text{Rx}} = 1.0 \text{ }\mu\text{H}, \quad M = 0.6 \text{ }\mu\text{H}. \quad (2.1.2)$$

## 2.2 Analytical results

In this section, we aim to validate the simulation results using analytical formulae. Therefore, let us assume geometry identical to the 3D CAD model depicted in Figure 2.1. This model features two inductors made of annealed copper, both with the same initial radius 10 mm and linear radius change of 1.46 mm per turn, and differing only in the number of turns. The transmitting coil has got  $N_{\text{Tx}} = 10$  turns, whereas the receiving coil has got only  $N_{\text{Rx}} = 5$  turns.

### 2.2.1 Resistance

The DC resistance  $R$  of a wire of uniform cross-sectional area  $A$ , length  $\ell$  and resistivity  $\rho$ , can be calculated using the renowned formula

$$R = \frac{\rho \ell}{A} = \frac{\ell}{\sigma A}, \quad (2.2.1)$$

where  $\sigma$  is conductivity, the reciprocal of resistivity. Thus, in order to calculate this value, we need to find the lengths of the wires constituting the respective coils. Since we already know their spiral geometry parameters, we can write their corresponding formulas using the spiral equation

$$r(\theta) = 10 + \frac{1.46}{2\pi}\theta, \quad 0 \leq \theta \leq N \cdot 2\pi, \quad (2.2.2)$$

where  $N$  is the number of turns of the individual spiral. Following this, we can recall the theorem from real analysis for calculating the arc length of a graph in a polar coordinate system which goes as follows:

**Theorem 2.2.1.** *Let  $f$  be a real function of class  $C^1$  on  $(\alpha, \beta)$ , where  $\alpha < \beta$ . The arc length of the graph of  $r = f(\theta)$  from  $\theta = \alpha$  to  $\theta = \beta$  is*

$$\ell = \int_{\alpha}^{\beta} \sqrt{|f(\theta)|^2 + |f'(\theta)|^2} d\theta = \int_{\alpha}^{\beta} \sqrt{r^2 + \left(\frac{\partial r}{\partial \theta}\right)^2} d\theta. \quad (2.2.3)$$

Substituting  $N = 10$  for the transmitting coil and  $N = 5$  for the receiving coil into Equation 2.2.2, we obtain the spiral equations

$$r_{\text{Tx}}(\theta) = 10 + \frac{1.46}{2\pi}\theta, \quad 0 \leq \theta \leq 10 \cdot 2\pi \quad (2.2.4)$$

---

<sup>1</sup>The inductance values can be computed for DC excitation in the *Magnetostatic solver* or for an arbitrary number of frequency points using the *EddyCurrent solver*. These two solvers were found to yield identical results in the DC case.



and

$$r_{\text{Rx}}(\theta) = 10 + \frac{1.46}{2\pi}\theta, \quad 0 \leq \theta \leq 5 \cdot 2\pi, \quad (2.2.5)$$

Furthermore, applying Theorem 2.2.1, we can calculate the lengths of the spirals as

$$\ell_{\text{Txs}} = \int_0^{10 \cdot 2\pi} \sqrt{\left(10 + \frac{1.46}{2\pi}\theta\right)^2 + \left(\frac{1.46}{2\pi}\right)^2} d\theta \text{ mm} \approx 1087.1 \text{ mm}, \quad (2.2.6)$$

$$\ell_{\text{Rxs}} = \int_0^{5 \cdot 2\pi} \sqrt{\left(10 + \frac{1.46}{2\pi}\theta\right)^2 + \left(\frac{1.46}{2\pi}\right)^2} d\theta \text{ mm} \approx 428.9 \text{ mm}. \quad (2.2.7)$$

For the total length of a coil, the feeding terminals must be taken into account:

$$\ell_{\text{TxT1}} = 94.0 \text{ mm}, \quad \ell_{\text{RxT1}} = 94.0 \text{ mm}, \quad (2.2.8)$$

$$\ell_{\text{TxT2}} = 86.7 \text{ mm}, \quad \ell_{\text{RxT2}} = 79.5 \text{ mm}. \quad (2.2.9)$$

Hence, the final length of the transmitting and receiving coils are

$$\ell_{\text{Tx}} = \ell_{\text{Txs}} + \ell_{\text{TxT1}} + \ell_{\text{TxT2}} = 1267.8 \text{ mm}, \quad (2.2.10)$$

$$\ell_{\text{Rx}} = \ell_{\text{Rxs}} + \ell_{\text{RxT1}} + \ell_{\text{RxT2}} = 602.4 \text{ mm}. \quad (2.2.11)$$

At last, we can apply Equation 2.2.1 to our case of the IWPT coils which consist of copper wire of cross-sectional area  $A = 1 \text{ mm}^2$ . The conductivity of annealed copper is  $\sigma = 5.8001 \times 10^7 \text{ S m}^{-1}$ . With lengths given by Equations 2.2.10 and 2.2.11, we obtain the values of DC resistance

$$R_{\text{Tx}} = 21.9 \text{ m}\Omega, \quad R_{\text{Rx}} = 10.4 \text{ m}\Omega. \quad (2.2.12)$$

Comparing these values with the simulation results contained in Equation 2.1.1, we can confirm the accuracy of the simulation to  $\approx 0.2 \text{ m}\Omega$ .

## 2.2.2 Inductance

The values of DC inductances, both self and mutual, are subject to complex computations using elliptic integrals. Luckily, we can utilize the astounding work [3] which provides us with an elaborate guide on how to determine the self and mutual inductance of coaxial coils in air. Furthermore, the aforementioned work was supplemented with numerical software [2] which performs all the complex calculations in response to simple input. This input is the task geometry:

### Transmitting coil:

- inner diameter: 20 mm,
- outer diameter: 51 mm,
- coil height: 1 mm,
- number of turns: 10.

### Receiving coil:

- inner diameter: 20 mm,
- outer diameter: 36 mm,
- coil height: 1 mm,
- number of turns: 5.

The axial coil distance is 10 mm. Using the fifth Romberg extrapolation  $R(n, 5)$  for estimation of the elliptic integrals, we obtain the values of inductance

$$L_{\text{Tx}} = 3.8 \text{ }\mu\text{H}, \quad L_{\text{Rx}} = 0.9 \text{ }\mu\text{H}, \quad M = 0.6 \text{ }\mu\text{H}. \quad (2.2.13)$$

Again, comparing these values with the simulation results in Equation 2.1.2, we can confirm the accuracy of the simulation to  $\approx 0.1 \text{ }\mu\text{H}$ .

# Conclusion

In summary, this thesis project has effectively demonstrated the capabilities of Maxwell ANSYS software in simulating and analyzing Inductive Wireless Power Transfer (IWPT) systems. Beginning with an introductory overview of IWPT systems and equivalent circuit models in Chapter 1, followed by a detailed simulation of basic coupled inductors in Chapter 2, we have established the software's reliability in capturing the electromagnetic behavior of such systems. The satisfactory agreement between simulated results and analytical formulas reaffirms the accuracy and robustness of Maxwell ANSYS, particularly in modeling IWPT systems with frequency dependencies and complex structures. These findings highlight the software's potential for designing and optimizing wireless power transfer technologies for practical applications. As we continue to refine simulation techniques and explore more sophisticated system configurations, the insights gained from this project will serve as a valuable foundation for future developments in the field.

# Bibliography

- [1] J. Kracek and M. Mazanek. Power balance of inductive wireless power transmission. *Proceedings of the 5th European Conference on Antennas and Propagation, EUCAP 2011*, 01 2011.
- [2] V. Pankrác. Software for self and mutual inductance calculation of coaxial coils in air. <https://elmag.fel.cvut.cz/uzivatel/vitezslav-pankrac/>.
- [3] V. Pankrác. Power inductors (part 3). *Elektrorevue*, 12(1):1–15, 2010. ISSN 1213–1539.